Inorganic Chemistry

Article

pubs.acs.org/IC

Octanuclear Zinc Phosphates with Hitherto Unknown Cluster Architectures: Ancillary Ligand and Solvent Assisted Structural Transformations Thereof

Aijaz A. Dar, Saumik Sen, Sandeep K. Gupta, G. Naresh Patwari, and Ramaswamy Murugavel*

Department of Chemistry, Indian Institute of Technology Bombay, Powai, Mumbai-400076, India

Supporting Information

ABSTRACT: Structural variations in zinc phosphate cluster chemistry have been achieved through a careful selection of phosphate ligand, ancillary ligand, and solvent medium. The use of 4-haloaryl phosphates (X-dippH$_2$) as phosphate source in conjunction with 2-hydroxypyridine (hpy) ancillary ligand in acetonitrile solvent resulted in the isolation of the first examples of octameric zinc phosphates [Zn$_8$(X-dipp)$_8$(hpy)$_4$(CH$_3$CN)$_2$(H$_2$O)$_2$]·4H$_2$O (X = Cl **2**, Br **3**) and not the expected tetranuclear D4R cubane clusters. Use of 2,3-dihydroxypyridine (dhpy) as ancillary ligand, under otherwise similar reaction conditions with the same set of phosphate ligands and solvent, resulted in isolation of another type of octanuclear zinc phosphate clusters {[(Zn$_8$(X-dipp)$_4$(X-dippH)$_4$(dhpyH)$_4$(dhpyH$_2$)$_2$(H$_2$O)$_2$]·2solvent} (X = Cl, solvent = MeCN **4**; Br, solvent = H$_2$O **5**), as the only isolated products. X-ray crystal diffraction studies reveal that **2** and **3** are octanuclear clusters that are essentially formed by edge fusion of two D4R zinc phosphates. Although **4** and **5** are also octanuclear clusters, they exhibit a completely different cluster architecture and have been presumably formed by the ability of 2,3-dihydroxypyridine to bridge zinc centers in addition to the X-dipp ligands. Dissolution of both types of octanuclear clusters in DMSO followed by crystallization yields D4R cubanes [Zn(X-dipp)(DMSO)]$_4$ (X = Cl **6**, Br **7**), in which the ancillary ligands such as hpy, H$_2$O, and CH$_3$CN originally present on the zinc centers of **2**−**5** have been replaced by DMSO. DFT calculations carried out to understand the preference of Zn$_8$ versus Zn$_4$ clusters in different solvent media reveal that use of CH$_3$CN as solvent favors the formation of fused cubanes of the type **2** and **3**, whereas use of DMSO as the solvent medium promotes the formation of D4R structures of the type **6** and **7**. The calculations also reveal that the vacant exocluster coordination sites on the zinc centers at the bridgehead positions prefer coordination by water to hpy or CH$_3$CN. Interestingly, the initially inaccessible D4R cubanes [Zn(X-dipp)(hpy)]$_4$·2MeCN (X = Cl **8**, Br **9**) could be isolated as the sole products from the corresponding DMSO-decorated cubanes **6** and **7** by combining them with hpy in CH$_3$CN.

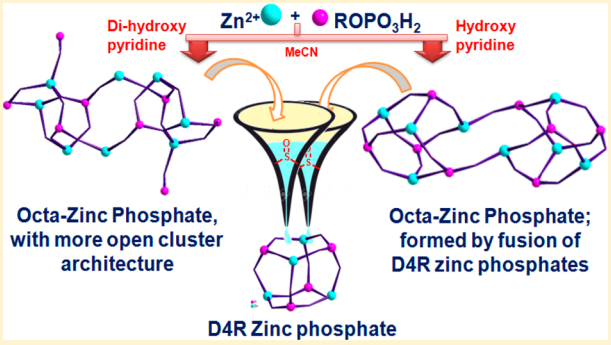

1. INTRODUCTION

In a quest to prepare novel porous materials other than zeolites, synthesis and studies on metallophosphates have witnessed fevered research activity during the last three to four decades,[1] primarily owing to the close structural resemblance of these materials to several naturally occurring as well as synthetic aluminosilicates. These materials serve efficiently in the areas of catalysis,[2] ion exchange,[3] adsorption,[4] matrices for electronic devices,[5] photoluminescence,[6] medicine,[7] proton conduction,[8] and gas storage and magnetism.[9] Zinc phosphates, a prime class within the family of metallophosphates, display a large structural variety and exist mostly as extended frameworks of various dimensionalities bearing large pores and low densities.[10−15] The molecular zinc phosphates on the other hand are relatively rare and are of recent origin. They have been implicated as useful candidates for biomimicking of nucleases and hydrolases/phosphatases.[1b] Owing to the recent realization that extended metallophosphates can be hierarchically built from molecular entities, discrete molecular zinc phosphates have received attention in recent times,[16] resulting in the isolation of di-,[17] tetra-,[16,18,19] hepta-,[20] and dodecanuclear[21] molecular zinc phosphates. In addition to the glaring absence of octa-zinc phosphates in the literature, there have also been no systematic investigations on the postsynthetic functionalization or cluster-to-cluster transformations of these polynuclear zinc phosphates. In this context, introduction of additional functional groups on the organic peripheral part of the zinc organophosphates can provide ample scope for postsynthetic modifications.

Although rational synthetic routes to metallophosphates have not been well established, available empirical studies suggest that the structure and nuclearity of these compounds can be varied (if not controlled) by altering ancillary ligands and/or reaction conditions.[19,22] For example, recent investigations have shown that tetranuclear zinc phosphates with a D4R core can

Received: June 10, 2015
Published: September 14, 2015

DOI: 10.1021/acs.inorgchem.5b01308
Inorg. Chem. 2015, 54, 9458−9469

be readily converted into supramolecular aggregates in the presence of appropriate ancillary ligands.[19a] Similarly, structural variations can be induced by varying ancillary ligands even in the case of manganese, copper, and iron phosphates.[19b−d] It has been further established in one instance that the change of metal precursor from zinc acetate to zinc sulfate alters the cluster size (tetra- to trinuclear).[19e]

The present investigation is aimed at unraveling the effect of (a) solvent, (b) ancillary ligand, and (c) introduction of a halogen function on the organophosphate ligand in molecular zinc phosphate chemistry. Two series of hitherto unknown octanuclear zinc phosphates have become available by minor adaptations, whose formation and existence is based on the solvent medium used. Change of solvent leads to interesting transformations, leading to isolation of other types of zinc phosphates. The details of this investigation along with detailed DFT calculations to understand the subtle energetic preferences involved in these systems are reported in this contribution.

2. RESULTS AND DISCUSSION

2.1. Reactivity of Zinc Acetate with X-dippH$_2$ in the Presence of 2-Hydroxypyridine. Earlier work from our laboratory has established that divalent first-row transition metal ions such as Cu, Co, Mn, and Zn undergo facile reaction with 2,6-diisopropylphenyl phosphate (dippH$_2$) in the presence of a pyridine-based ancillary ligand (AL) at room temperature in *methanol* to produce tetranuclear metal phosphates of the formula [M(dipp)(AL)]$_4$, which normally exists as a cubane cluster resembling the D4R secondary building units of zeolites.[9,19,23] Especially in the case of zinc, the scope of the AL has been well tested, leading to the isolation of a large number of compounds with the D4R cluster architecture.[19] One specific example is the reaction of zinc acetate and dippH$_2$ in the presence of ancillary ligand 2-hydroxypyridine (hpy) in methanol to yield [Zn(dipp)(hpy)]$_4$ (**1**) (Scheme 1).[19a] Interestingly, hpy

Scheme 1. Synthesis of 1

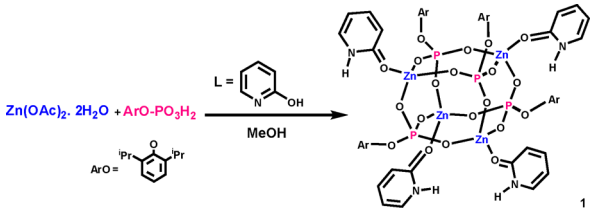

binds to zinc centers in **1** through the oxygen rather than pyridinic nitrogen due to hydroxypyridine−pyridone tautomerism. This results in the −NH groups on the cubane clusters engaging themselves in both intra- and intercubane hydrogen bonds with oxygen centers of the phosphate ligands, thereby leading to formation of a supramolecular 2-D H-bonded framework structure for **1** in the solid state.

In a more recent study, it has been demonstrated that 4-halo-2,6-diisopropylphenyl phosphates (X-dippH$_2$; X = Cl, Br, I) exhibit a different type of reactivity compared to the parent dippH$_2$ for reactions carried out under similar reaction conditions.[19f] This prompted us to investigate the reactions of X-dippH$_2$ with zinc acetate especially in the presence of hydroxylpyridines, which as described above can coordinate either through oxygen or nitrogen centers, and see whether zinc phosphates with cluster architecture other than D4R can be isolated.

Consequently, the reactions of zinc acetate with X-dippH$_2$ using hpy as the ancillary ligand were carried out in methanol under reaction conditions similar to those employed for the isolation of **1**. These reactions however did not proceed cleanly to produce hpy-decorated D4R cubanes (Scheme 2; eq 1). Efforts to obtain crystalline products from the reaction mixture did not yield desired results, necessitating changes in the reaction conditions, viz., the solvent medium. On change of solvent to acetonitrile, these reactions involving a 1:1:1 ratio of the three reactants Zn(OAc)$_2$·2H$_2$O, X-dippH$_2$, and hpy were found to proceed smoothly and produce zinc phosphates [Zn$_8$(X-dipp)$_8$(hpy)$_4$(CH$_3$CN)$_2$(H$_2$O)$_2$]·4H$_2$O (X = Cl **2**, Br **3**) (Scheme 2; eq 2). Owing to the poor solubility in most of the common organic solvents (other than DMSO), the crystalline products **2** and **3** have been characterized by various solid-state analytical and spectroscopic methods.

The absence of any absorption at around 2350 cm^{-1} in the FT-IR spectra in **2** and **3** indicates complete deprotonation of the halo-arylphosphate ligands, leaving no residual P-OH group in the ligands. The absorption bands appearing at 3270 and 3240 cm^{-1} in the FT-IR spectrum of **2** or **3**, respectively, indicate the migration of the hydroxyl proton of the hpy ligand to the neighboring nitrogen center. Sharp absorption bands appearing at 1165, 1021, and 923 cm^{-1} for **2** and at 1185, 1041, and 930 cm^{-1} for **3** can be attributed to the O−P−O stretching and M−O−P asymmetric and symmetric stretching vibrations, respectively (SI). The DMSO solution and solid-state ^{31}P NMR spectroscopic data of **2** (as well as the ESI-mass spectral data in DMSO) are suggestive of the presence of completely different species in the two different states of matter (*vide infra*). Hence the solid-state structures of both **2** and **3** have been determined by single-crystal X-ray diffraction studies to unravel their definitive structures.

2.2. Molecular Structures of 2 and 3. X-ray diffraction quality single crystals of **2** and **3** have been obtained directly from the reaction mixture by slow evaporation of acetonitrile solution at room temperature after a period of 3−4 days. The isomorphic compounds **2** and **3** crystallize in the tetragonal space group $I4_1/a$. Change of phosphate source to X-dippH$_2$ and solvent medium to acetonitrile brings about the anticipated major change in the nuclearity and structure of the final product through the isolation of the octanuclear zinc phosphates **2** and **3** (Figure 1). To the best of our knowledge, **2** and **3** represent the first examples of octanuclear zinc phosphates.

Zinc phosphate **2** is built from eight zinc dications and eight haloaryl phosphate dianions, producing a [Zn$_8$P$_8$O$_{24}$] inorganic polyhedral core that has been fully enveloped by an organic periphery comprising halo-2,6-diisopropylphenyl groups and the ancillary ligands. The inorganic core in **2** can be regarded as the product of a fusion of two commonly isolated D4R tetranuclear phosphates. The fusion presumably occurs through the opening of one of the edges (P3−O11−Zn3) of each D4R cubane followed by formation of (P3−O11−Zn3′) double bridges across the two cages (Scheme 3). Each of the eight zinc centers in **2** are tetracoordinate and are bound by three phosphate oxygen atoms of three different phosphate ligands. In other words, each phosphate ligand embraces three different zinc ions, exhibiting a Harris [3.111] mode of coordination behavior.[24] The fourth coordination site on each tetrahedral zinc center is occupied by an exocage ancillary ligand. Although an adequate amount of hpy ligand has been used in the reaction, not all eight zinc centers are capped by hpy ligands; the zinc centers right on the bridge between the two D4R units

DOI: 10.1021/acs.inorgchem.5b01308
Inorg. Chem. 2015, 54, 9458−9469

Scheme 2. Synthesis and Structural Modulations of Zinc Phosphates 2−9

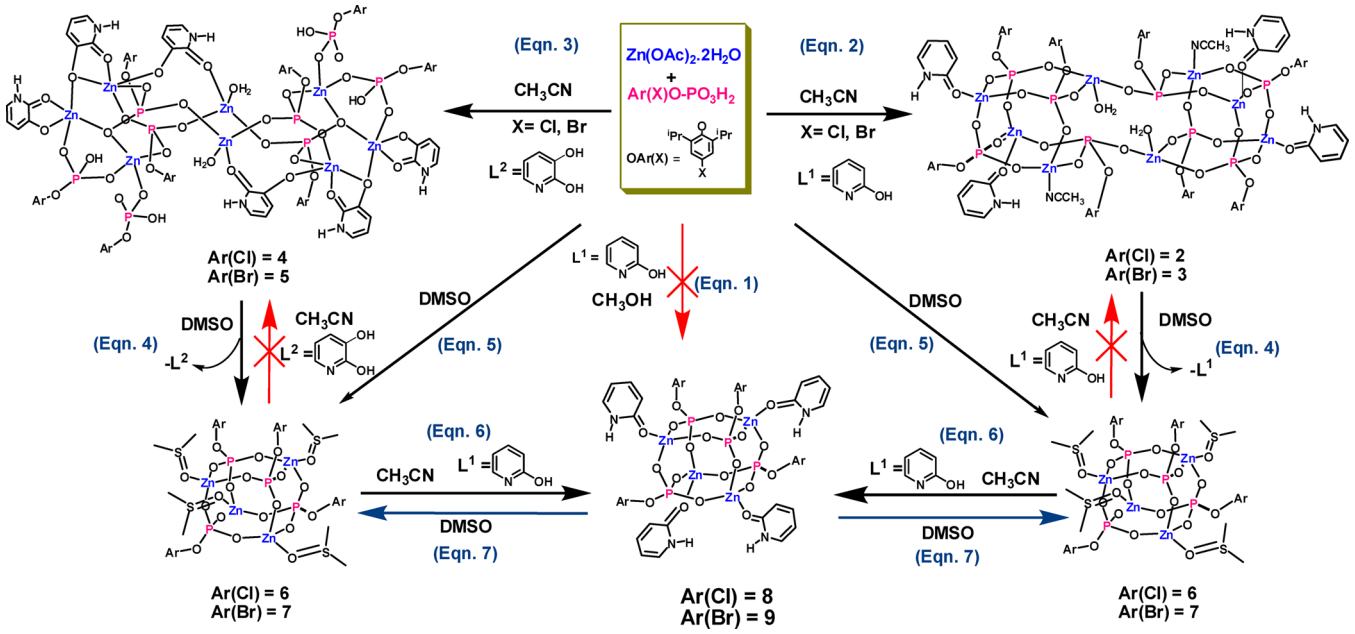

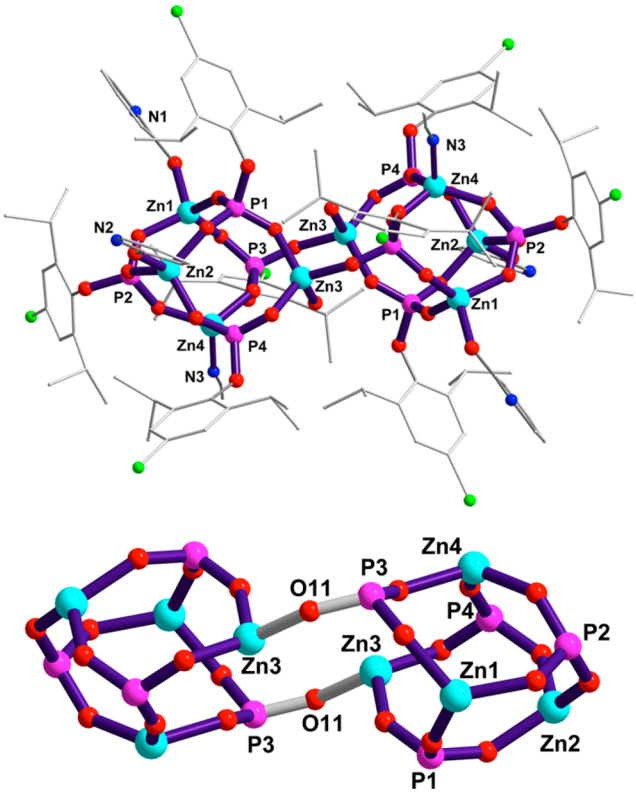

Figure 1. (a) Molecular structure of compound **2**. (b) Inorganic core of **2** highlighting the bridges between two D4R rings (gray bonds). Zinc and phosphorus centers are tetrahedral, average bond angles (deg): 109.17 (Zn1), 109.94 (Zn2), 109.16 (Zn3), 109.29 (Zn4), 109.29 (P1), 109.30 (P2), 109.34 (P3), and 109.34 (P4) for **2**; 109.46 (Zn1), 109.20 (Zn2), 109.16 (Zn3), 109.31 (Zn4), 109.32 (P1), 109.33 (P2), 109.33 (P3), and 109.34 (P4) for **3**.

(Zn3 and Zn3′) are coordinated by water, while Zn4 and Zn4′, which are close to the bridge between the D4R units, are coordinated by acetonitrile as ancillary ligand. The four zinc centers that are farther from the center of the cluster (Zn1, Zn1′, Zn2, and Zn2′) are bound by hpy ligands in the pyridone form. It appears that during the course of the reaction all three ancillary ligands (hpy, water, and acetonitrile) are available for coordination, and the zinc ions, depending upon their position in the cluster (i.e., closer to or farther from the bridge between the two D4R units), may have preference for one of these ligands over the other.

The average P−O(Zn) bond length in the core in **2** is 1.506 Å (1.508 Å in **3**); these values are closer to P═O double-bond distances (P−O 1.60 Å and P═O 1.45−1.46 Å).[25] The bridge across the two D4R units exhibits Zn−O−P angles of 145.38(1)° and 145.50(1)° for **2** and **3**, respectively. Intermolecular N−H···O hydrogen-bonding interactions between the adjacent clusters leads to the formation of three-dimensional supramolecular assemblies (SI). The coordinated water molecules additionally undergo strong intramolecular hydrogen bonding with the cluster phosphate oxygen and, hence, afford additional stabilization to the extended octanuclear inorganic core (SI).

2.3. Reactivity of Zinc Acetate with X-dippH$_2$ in the Presence of 2,3-Dihydroxypyridine. The observation that, instead of pyridinic nitrogen atom, the hydroxyl oxygen atom of hpy ancillary ligands coordinates to zinc centers in **2** and **3** prompted the investigation of the effect of a pyridinic ligand that contains more than one hydroxyl group. 2,3-Dihydroxypyridine (dhpy), chosen for this purpose with the expectation that the additional hydroxyl group can either chelate and/or bridge proximal zinc centers, affords a second series of octanuclear zinc phosphates {[(Zn$_8$(X-dipp)$_4$(X-dippH)$_4$(dhpyH)$_4$(dhpyH$_2$)$_2$(H$_2$O)$_2$]·2solvent} (X = Cl, solvent = MeCN **4**, Br, solvent = H$_2$O **5**) under identical reaction conditions described above to synthesize **2** and **3** (Scheme 2, eq 3). While the clusters are freely soluble in DMSO, they have been found to be insoluble in other organic solvents. The presence of a broad absorption at around 2350 cm^{-1} in the FT-IR spectrum of either **4** or **5** indicates the presence of residual P−OH groups of halo-aryl phosphates. As in the case of **2** and **3**, the liquid-state ^{31}P NMR spectra in DMSO and the solid-state spectrum are

DOI: 10.1021/acs.inorgchem.5b01308
Inorg. Chem. 2015, 54, 9458−9469

Scheme 3. Opening up of One of the Zn−O−P Edges of D4R Cubanes and Subsequent Bridge Formation across the Cubanes Leading to Octameric Zinc Phosphates

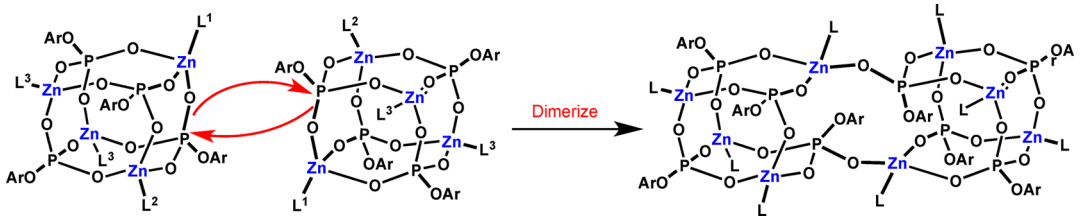

completely different, suggesting that these clusters exhibit a different structure in DMSO (see below).

2.4. Molecular Structure of 4 and 5. X-ray quality single crystals of **4** and **5** have been directly obtained from the reaction mixture by slow evaporation of solvent at room temperature after about 1 week. Compounds **4** and **5** are isostructural and crystallize in the orthorhombic space group, *Pbca*. A perspective view of the molecular structure and its inorganic core revealing the octanuclear aggregation of zinc centers in **4** is shown in Figure 2 (for **5** see the SI). The asymmetric part of the unit cell consists of one-half of the molecule of **4**, which consists of four zinc ions, four phosphates, three dhpy, and a coordinated water molecule. In addition, there are two molecules of acetonitrile and water in the lattice of **4** and **5**, respectively. The zinc centers are chemically nonequivalent and adopt tetrahedral and trigonal bipyramidal geometries. Zn1 centers are in tetrahedral geometry, with bond angles around them ranging from 102.60(1)° to 116.51(1)° (av 109.26°) for **4** and 102.76(2)−117.56(2)° (av 109.35°) for **5**. The Zn2, Zn3, and Zn4 centers exhibit distorted trigonal-bipyramidal geometry. The halo-aryl phosphate ligands (denoted as P1, P2, P3, and P4 in Figure 2) in **4** and **5** exhibit diverse coordination behavior, as the four ligands in the asymmetric unit exhibit four different modes of coordination to the metal ion. For example, P1 is monodeprotonated and binds to a single metal ion (Zn1) as a terminal monodentate ligand (Harris notation [1.100]), while the other monoanionic phosphate ligand P2 bridges two metal centers (Zn1 and Zn3; Harris notation [2.110]). The dianionic P3 binds three different metal ions through three different oxygen centers and thus exhibits a [3.111] mode of binding. Although P4 is also dianionic, it binds to all four zinc ions in the asymmetric part where one of the three oxygen bridges two metal centers ([4.211] mode of binding) (see the SI for further details).[24] All the phosphorus centers are in tetrahedral geometry. The dhpy ancillary ligands undergo a proton shift similar to hpy in **2** and **3** and exist in zwitterionic form. Two of the three dhpy ligands in the asymmetric unit of **4** and **5** are monoanionic, while the third ligand is neutral. The anionic ancillary ligands chelate as well as bridge the zinc centers, while neutral ones act as chelating ligands and retain the proton on one of the coordinated oxygen atoms (SI).

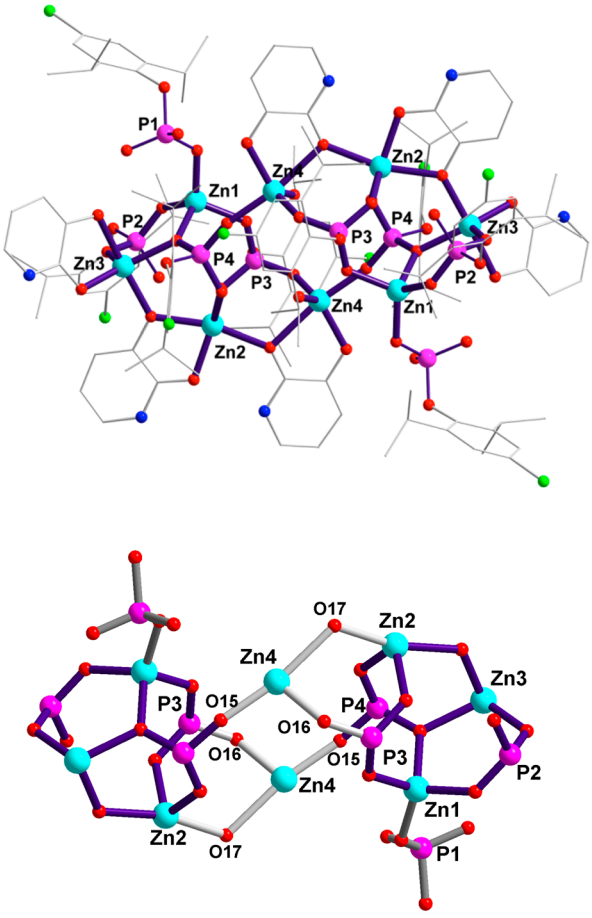

Figure 2. (a) Molecular structure of **4** (H atoms and lattice solvent molecules are omitted for clarity). (b) Inorganic core of **4** highlighting the similarity to fused and scrambled D4R cores.

The molecular complexes **4** and **5** are further stabilized by extensive intramolecular hydrogen bonding involving residual P−OH, P═O, O−H, and N−H groups on hydroxypyridine and phosphate ligands and coordinated water molecules. There are 12 intramolecular hydrogen-bonding interactions for cluster **4** (SI). The peripheral N−H protons of dhpy groups are not involved in any hydrogen-bonding interactions. Owing to the extensive hydrophobic sheath on the surface, there are no intermolecular hydrogen-bonding interactions in **4** and **5**, and thus they exist as discrete molecules and are held together by weak intermolecular forces.

2.5. Rearrangement of Octanuclear Zinc Phosphates to D4R Structures in DMSO Solution. As described above, the octanuclear zinc phosphates **2**−**5** are insoluble in most organic solvents except DMSO. The ^{1}H NMR spectra of **2** and **3** in DMSO show well-separated peaks for the protons of X-dipp and hpy with a peak integral ratio of 2:1 (SI). Interestingly, only a single resonance is observed in DMSO solution ^{31}P NMR spectra of **2** and **3** (δ −5.0 ppm) (Figure 3a). This is quite contrary to the different types of phosphorus centers observed in the crystal structure of **2** and **3**. The presence of just a single resonance at around $\delta_P \approx -5.0$ ppm for **2**−**5**, however, is not surprising in light of earlier observations that all previously reported D4R zinc phosphates exhibit a single resonance in DMSO-d_6 solution at the very same chemical shift.[9,19,23]

DOI: 10.1021/acs.inorgchem.5b01308
Inorg. Chem. 2015, 54, 9458−9469

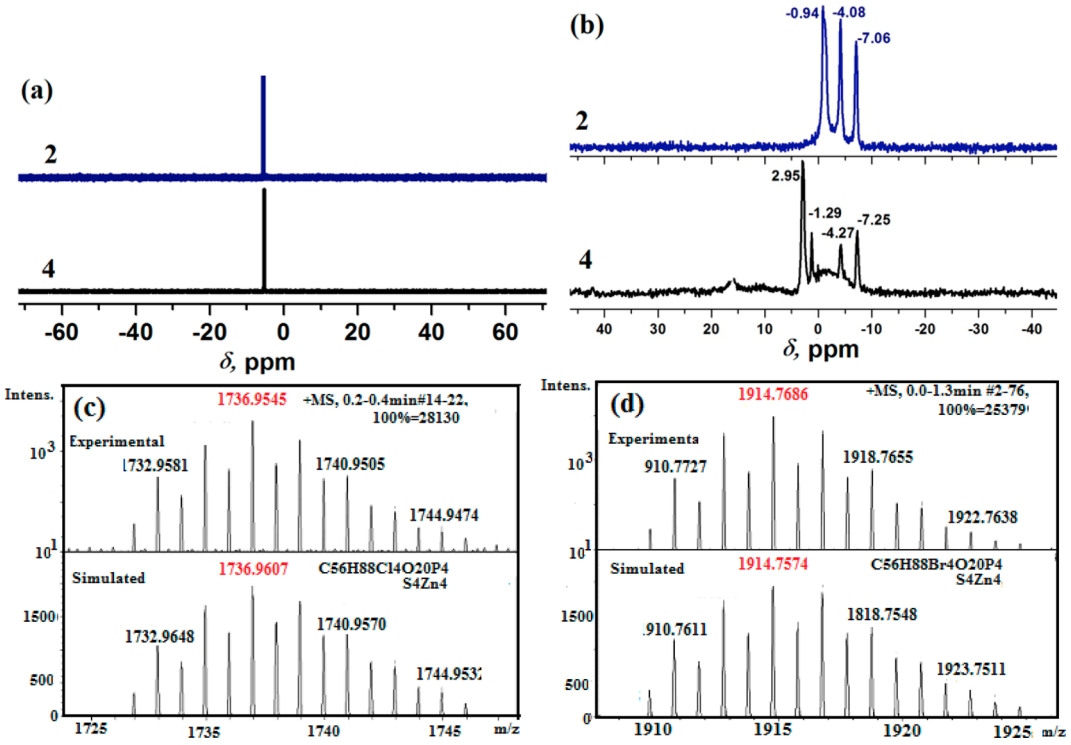

Figure 3. (a) Liquid-state ^{31}P NMR spectra of **2** and **4**; (b) CP-MAS ^{31}P NMR spectra of **2** or **4**; (c) ESI-MS spectra of of **2** or **4**; and (d) ESI-MS spectra of **3** or **5**.

In contrast to the DMSO-d_6 solution spectra of **2**−**5**, the solid-state structure analysis of these complexes have revealed that the phosphorus centers are chemically nonequivalent. Hence CP-MAS ^{31}P NMR spectral measurements of **2**−**5** have been carried out. The spectra of **2** and **3** exhibit three singlet resonances in the solid state, which can be readily assigned to three types of chemically nonequivalent phosphorus centers in these compounds (for **2**: δ −0.94 ppm for P3 and P4, δ −4.08 ppm for P2, and δ −7.06 ppm for P1) (Figure 3b). Similarly, for **4** and **5** four signals are observed for four types of chemically nonequivalent phosphorus centers (δ 2.95 ppm for P1, δ −1.29 ppm for P2, δ −4.27 ppm for P3, and δ −7.05 ppm for P4 centers) (Figure 3b) (also see the SI).

It emerges that the discrepancy between the solution and solid-state NMR studies of these compounds can be attributed to either a possible rearrangement or complete dissociation to the constituents in DMSO solution. ESI-MS studies of **2**−**5** carried out in DMSO clearly support the rearrangement process over complete dissociation. As it can be seen from Figure 3c, both **2** and **4**, in spite of the large differences in the structures of these molecules in the solid state (both prepared from Cl-dipp), produce spectra with identical isotope patterns for the peak at m/z 1736.95. Similarly both **3** and **5** exhibit identical spectral patterns for the peak at m/z 1914.76 (Figure 3d). These experimentally obtained m/z values can be readily assigned to D4R zinc phosphates $[\{Zn(Cl\text{-}dipp)(DMSO)\}_4+H]^+$ and $[\{Zn(Br\text{-}dipp)(DMSO)\}_4+H]^+$ (Figure 5), suggesting that the octanuclear phosphates rearrange in DMSO to more symmetrical tetranuclear D4R phosphates.

To further validate these observations, bulk quantities of **2**−**5** have been recrystallized from DMSO as single crystals and their solid-state structures have been established. Recrystallization of either **2** or **4** in DMSO under ambient conditions yields block-shaped crystals, whose solid-state structure confirms reorganization

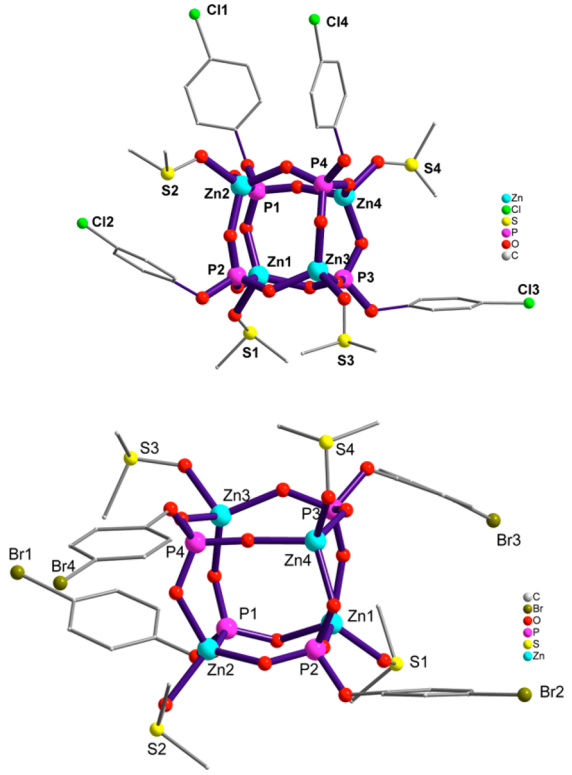

Figure 4. Molecular structure of compounds **6** and **7** (isopropyl groups of phosphate ligand, H atoms, and lattice solvent molecules are omitted for clarity).

of the octamers to more symmetrical D4R zinc phosphate $[Zn(Cl\text{-}dipp)(DMSO)]_4$ (**6**). Compound $\{[Zn(Br\text{-}dipp)(DMSO)]_4\cdot 4DMSO\}$ (**7**) has been similarly obtained by

DOI: 10.1021/acs.inorgchem.5b01308
Inorg. Chem. 2015, 54, 9458−9469

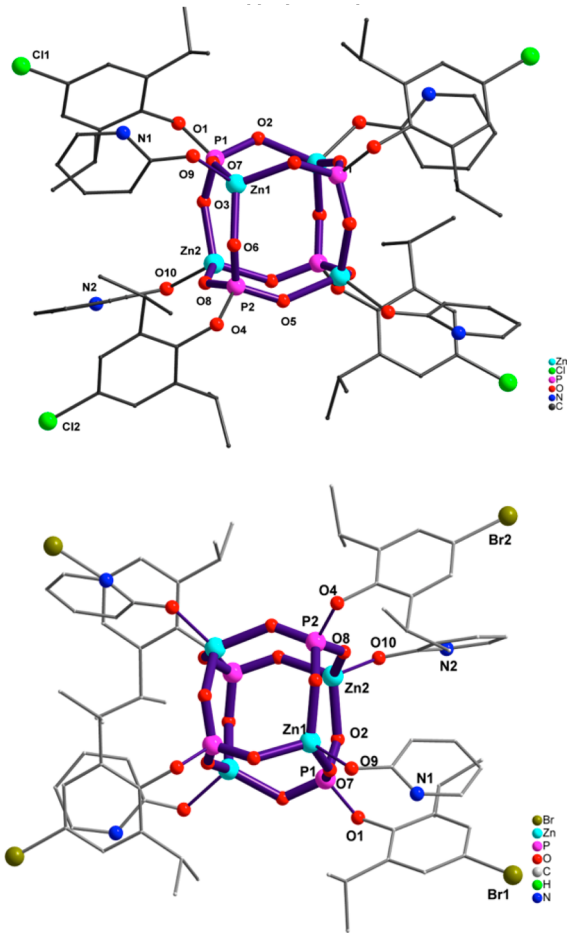

Figure 5. Molecular structure diagram of compounds **8** and **9** (H atoms are omitted for clarity).

recrystallization of **3** or **5** in DMSO (Scheme 2; eq 4). The direct reaction of the three primary starting materials, zinc acetate, X-dippH$_2$, and hpy, in DMSO also yielded **6** or **7** quantitatively, further supporting the role played by DMSO in keeping other donor ligands away from zinc ions and also keeping the cluster size as tetranuclear (Scheme 2; eq 5).

D4R clusters **6** and **7** have been characterized by spectroscopic and analytical methods. The absorption bands at 1184, 1023, and 922 cm^{-1} for **6** and at 1184, 1023, and 913 cm^{-1} for **7** are assigned to the O−P−O stretching vibrations and M−O−P asymmetric and symmetric stretching vibrations, respectively (SI). A single resonance at δ −5.5 or −5.6 ppm is observed in the liquid-state ^{31}P NMR spectra of **6** and **7**, respectively. The absence of an absorption band at around 3250 cm^{-1} in the FT-IR spectra and the presence of a broad resonance at around δ 11 ppm in the ^{1}H NMR spectra of **6** and **7** suggest the absence of hpy or dhpy ancillary ligands.

2.6. Molecular Structures of 6 and 7. Compounds **6** and **7** crystallize in monoclinic space groups *I*2/*a* and *P*2/*c*, respectively. These compounds are isostructural, consisting of the discrete tetranuclear D4R zinc phosphate core, Figure 4.

The vertices of these cubanes are alternately occupied by zinc and phosphorus centers, which are bridged by μ_2 oxygen atoms. Both zinc and phosphorus centers are in tetrahedral geometry. The bond parameters of these tetramers are similar and are comparable to earlier reported zinc phosphates with D4R architecture (Table 1). Unlike **6**, the crystal of **7** contains four DMSO molecules for every D4R cluster.

The average O−Zn−O bond angle values are 109.24° in **6** and 109.20° in **7**, while the average O−P−O bond angle values are 109.27° in **6** and 109.29° in **7**. Average Zn−O bond distances are 1.942 and 1.939 Å, while the average P−O bond distances are 1.534 and 1.532 Å in **6** and **7**, respectively. The Zn−O−P bond angles are in the ranges 128.40(1)−159.71(3)° and 121.77(2)−177.40(1)° in **6** and **7**, respectively. The dimensions of the cubic core in **6** and **7** can be best inferred from the distances of Zn···P edges, P···P face diagonals, Zn···Zn face diagonals, and Zn···P body diagonals, given in Table 1.

2.7. D4R Zinc Phosphates Decorated with 2-Hydroxypyridine. The formation of **6** (or **7**) clearly suggests that in DMSO solution D4R is the most favored cluster architecture for zinc phosphates with zinc ions exhibiting a strong preference for DMSO as the capping ancillary ligand, in spite of the presence of other ancillary ligands such as hpy or dhpy in the reaction medium. It will be of interest to probe weather these DMSO ligands are labile and would give way to hpy-type ligands to bind zinc centers in a solvent medium other than DMSO. For example, would addition of hpy to either **6** or **7** in acetonitrile lead to the formation of cubane clusters decorated with hpy ligands such as **8** or **9**, or would this lead to fusion of two different cubanes to form either **2** or **3**? To find out which of these two reactions are favored, **6** and **7** have been reacted with four equivalents of hpy in acetonitrile at room temperature and found to yield [Zn(X-dipp)(hpy)]$_4$·2MeCN (X = Cl **8**; Br **9**) (Scheme 2; eq 6) rather than the octanuclear clusters.

The reaction with dhpy ligands in acetonitrile under similar conditions yielded a light brown, insoluble gel. Products **8** and **9** have been characterized by spectroscopic and analytical methods (see Experimental Section), and their molecular structures have been confirmed by X-ray diffraction analyses. The ESI-MS spectra of **8** and **9** recorded in acetonitrile reveal the presence of molecular ions at *m*/*z* 1805.11 and 2004.97 mass numbers, corresponding to [M + H]$^+$ and [M + Na]$^+$, respectively.

2.8. Molecular Structures of 8 and 9. X-ray quality crystals of **8** and **9** have been directly obtained from the reaction mixture by slow evaporation of solvent over a period of 2−3 days. Single-crystal structure determination reveals that these compounds are isomorphous and crystallize in monoclinic space group *I*2/*a*. These compounds retain the tetranuclear inorganic core of **6** and **7** and undergo only peripheral substitution of coordinated DMSO molecules by hpy ligands, Figure 5. The tetrahedral zinc and phosphorus centers occupy alternate corners of the cubane core, and the coordinated hpy groups exist in zwitterionic pyridinium phenoxide form. The bond parameters of the D4R core in **8** and **9** are similar to those of **6** and **7** and other reported D4R zinc phosphates and are compared in Table 1.

Compounds **8** and **9** undergo extensive hydrogen bonding via N−H···O interactions. The N−H protons of all four ancillary ligands participate in intermolecular hydrogen bonding; two have the oxygen atoms of the aryloxides of two neighboring cubanes as acceptors (N1−H1N···O9) and the other two engage with oxygen atoms of the cubic framework of two neighboring cubanes as acceptors (N2−H2N···O3) (Figure 6). Each D4R molecule of **8** and **9** forms eight hydrogen bonds with four neighboring molecules, leading to the formation of a three-dimensional supramolecular aggregate (Figure 6).

DOI: 10.1021/acs.inorgchem.5b01308
Inorg. Chem. 2015, 54, 9458−9469

Table 1. Comparison of Structural Parameters of 2−9 with Each Other and Other Earlier Reported D4R Zinc Phosphates[a]

formula	cryst syst	space group	Zn−N [Å]	Zn−O [Å]	P−O [Å]	Zn···P [Å]	face diagonal Zn···Zn [Å]	face diagonal P···P [Å]	body diagonal [Å]	ref
$[Zn(dipp)(Coll)]_4$	tetragonal	$I4_1/a$	2.087	1.916	1.532	3.196	4.419	4.632	5.529	19a
$[Zn(dipp)(pyridine)]_4$	triclinic	$P\bar{1}$	2.029	1.918	1.537	3.166	4.318	4.625	5.476	19a
$[Zn(dipp)(2\text{-apy})]_4$	monoclinic	$C2c$	2.027	1.923	1.537	3.179	4.347	4.598	5.477	19a
$[Zn(Cl\text{-}dipp)(Coll)]_4$	tetragonal	$I\bar{4}$	2.079	1.921	1.491	3.197	4.471	4.527	5.536	19f
$[Zn(Br\text{-}dipp)(Coll)]_4$	triclinic	$P1$	2.085	1.931	1.512	3.212	4.482	4.483	5.542	19f
$[Zn(Cl\text{-}dipp)(2apy)]_4$	triclinic	$P1$	2.020	1.933	1.511	3.175	4.447	4.541	5.544	19f
$[Zn(Br\text{-}dipp)(2apy)]_4$	orthorhombic	$P2_12_12$	2.015	1.925	1.507	3.172	4.448	4.553	5.521	19f
$[Zn_8(Cl\text{-}dipp)_8(hpy)_4(CH_3CN)_2(H_2O)_2]\cdot 4H_2O$ (**2**)	tetragonal	$I4_1/a$	1.992	1.936	1.526	3.201				this work
$[Zn_8(Br\text{-}dipp)_8(hpy)_4(CH_3CN)_2(H_2O)_2]\cdot 4H_2O$ (**3**)	tetragonal	$I4_1/a$	1.994	1.926	1.536	3.162				this work
$[(Zn_8(Cl\text{-}dipp)_4(X\text{-}dippH)_4(dhpyH)_4(dhpyH_2)_2(H_2O)_2]\cdot 2MeCN$ (**4**)	orthorhombic	$Pbca$		1.998	1.539					this work
$[(Zn_8(Br\text{-}dipp)_4(X\text{-}dippH)_4(dhpyH)_4(dhpyH_2)_2(H_2O)_2]\cdot 2H_2O$ (**5**)	orthorhombic	$Pbca$		1.985	1.532					this work
$[Zn(Cl\text{-}dipp)(DMSO)]_4$ (**6**)	monoclinic	$I2/a$		1.928	1.528	3.145	4.356	4.623	5.529	this work
$[Zn(Br\text{-}dipp)(DMSO)]_4\cdot 4DMSO$ (**7**)	monoclinic	$P2c$		1.944	1.523	3.195	4.391	4.653	5.384	this work
$[Zn(Cl\text{-}dipp)(hpy)]_4\cdot 2MeCN$ (**8**)	monoclinic	$I2/a$		1.930	1.529	3.196	4.327	4.623	5.413	this work
$[Zn(Br\text{-}dipp)(hpy)]_4\cdot 2MeCN$ (**9**)	monoclinic	$I2/a$		1.925	1.535	3.206	4.335	4.691	5.553	this work

[a]Average values of bond lengths are reported.

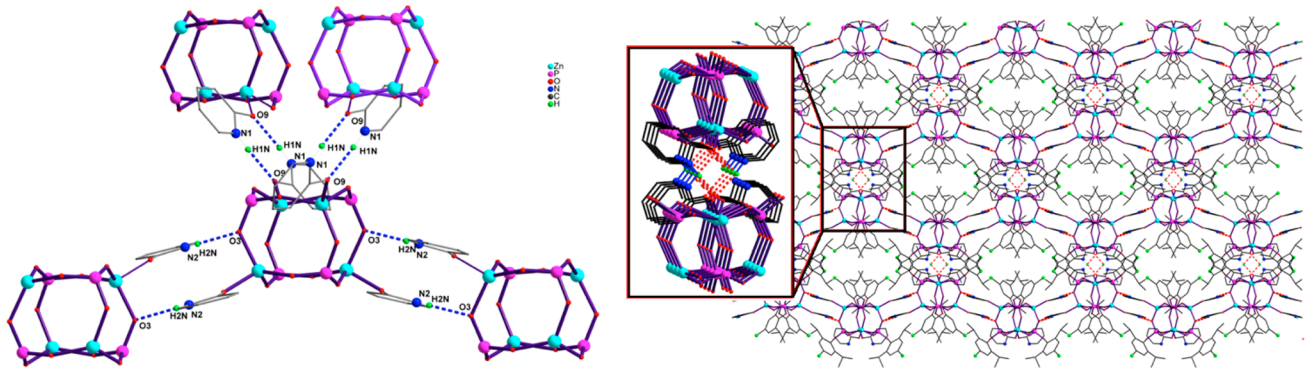

Figure 6. Intermolecular hydrogen-bonding diagram of **8**. Hydrogen bond lengths [Å] and angles [deg]: N1−H1N···O9 2.885(2) and 175.32(1); N2−H2N···O3 2.875(4) and 148.29(1). (b) Packing diagram of **8**.

As has been anticipated, **8** and **9** on treatment with excess DMSO/recrystallization from DMSO yielded back **6** and **7** as block-shaped crystals in good yields (Scheme 2, eq 7).

2.9. Summary and DFT Studies. The experimental observations described in Scheme 2 clearly favor the following: (a) direct reaction involving zinc acetate, X-dippH$_2$, and hpy or dhpy *in methanol* does not yield the D4R cluster decorated by hpy or dhpy ligands (eq 1), as one would normally expect based on the earlier reported reactions involving unsubstituted dippH$_2$;[19a] (b) the change of solvent to *acetonitrile* favors the formation of hitherto unknown octanuclear cluster **3** or **4**, which are essentially side-by-side fusion products of D4R clusters (eq 2); (c) DMSO splits the octanuclear clusters to tetrameric clusters **6** and **7**, also substituting all ancillary ligands by DMSO (eq 4); (d) **6** and **7** can be treated with hpy in acetonitrile to yield hpy-decorated H-bonded framework structures **8** and **9** without any trace of dimerization back to octanuclear clusters.

While the experimental facts have been reported in this contribution so far, it would be interesting to investigate the energetics behind the structural diversity and preferences for solvents and/or ancillary ligands. In order to explain these preferences, density functional theory (DFT) energy calculations have been carried out both in the gas phase and in solution (PCM calculations). In order to facilitate the complete geometric optimization of such large clusters in reasonable time periods, the model compounds **A** (for octanuclear compounds) and **B** (for tetranuclear compounds) have been chosen, where essentially all OAr groups have been truncated to OMe and in dimeric clusters hpy ligands have been replaced by MeOH (Figure 7). From a large number of calculations carried out on different **A** and **B**, four different useful comparisons have been extracted, which are listed in Tables 2−5.

It is evident from Table 2 that, when CH_3CN is used as the solvent, it is energetically favored for the aqua ligand to bind zinc ions on the bridges (i.e., H_2O as L_2) rather than having both L_1 and L_2 the same as the solvent (entry 1; stabilization by 16.3 kJ/mol). When MeOH is used as the solvent, this stabilization is not that appreciable, as in the case of CH_3CN (2.6 kJ/mol), although the molecule still prefers water as L_2. However, when DMSO is the choice of solvent, if dimeric structure **A** were to form, there appears to be a huge destabilization by 21.8 kJ/mol if water binds as L_2. Although trends for energies obtained both in the gas phase and in solution listed in Table 2 are similar, the gas-phase calculations appear to overestimate the difference.

DOI: 10.1021/acs.inorgchem.5b01308
Inorg. Chem. 2015, 54, 9458−9469

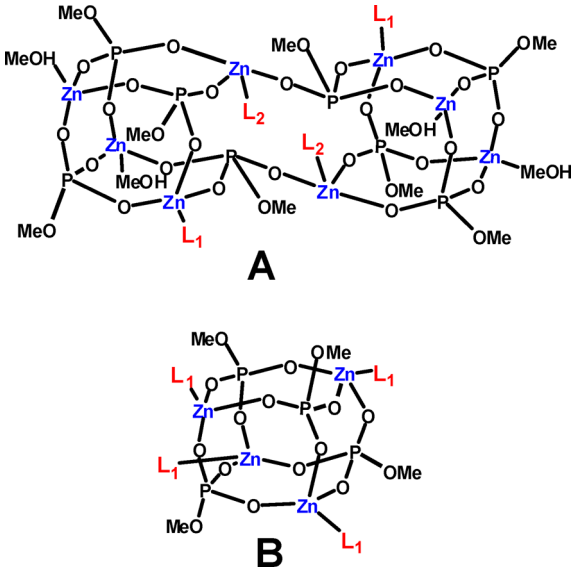

Figure 7. Model systems **A** and **B** with different L_1 and L_2 ligands used for DFT calculations.

Table 2. Relative Energies (kJ/mol) of A for Various L_1 and L_2 in the Gas Phase and Solution Phase Showing the Preference for L_2 To Be H_2O Irrespective of Whether L_1 Is CH_3CN, DMSO, or CH_3OH

entry	structures	gas phase	solution phase
1	$L_1 = CH_3CN$, $L_2 = H_2O$	0.0	0.0
	$L_1 = L_2 = CH_3CN$	15.8	16.3
2	$L_1 = CH_3OH$, $L_2 = H_2O$	0.0	0.0
	$L_1 = L_2 = CH_3OH$	26.8	2.6
3	L_1 = DMSO, $L_2 = H_2O$	151.0	21.8
	$L_1 = L_2$ = DMSO	0.0	0.0

Table 3. Relative Energies (kJ/mol) of A for Various L_1 Showing the Preference for CH_3CN in the Solution Phase and DMSO in the Gas Phase

entry	structures	gas phase	solution phase
1	$L_1 = CH_3CN$, $L_2 = H_2O$	29.2	0.0
2	$L_1 = CH_3OH$, $L_2 = H_2O$	40.7	127.8
3	L_1 = DMSO, $L_2 = H_2O$	0.0	7.2

Table 4. Relative Energies (kJ/mol) of B for Various L_1 Showing the Stabilization of Form B in DMSO

entry	structures	gas phase	solution phase
1	$L_1 = CH_3CN$	45.9	3.1
2	$L_1 = CH_3OH$	40.0	31.5
3	L_1 = DMSO	0.0	0.0

Table 5. Energetics (kJ/mol) of Form A versus Form B for the Isolated Species

entry	structures	gas phase	solution phase
1	$L_1 = CH_3CN$, $L_2 = H_2O$ (fused cubes)	39.9	24.9
	L_1 = DMSO (cube)	0.0	0.0
2	$L_1 = L_2$ = DMSO (fused cubes)	829.8	356.4
	L_1 = DMSO (cube)	0.0	0.0

Calculations carried out to find out in which solvent the D4R form (**B**) is preferentially stabilized indicate that DMSO is clearly favored as ancillary ligand or reaction medium in both the gas and solution phases (Table 4). Finally, the comparison of the **A** form with $L_1 = CH_3CN$ and $L_2 = H_2O$ (models for isolated compounds **2** and **3**) with the **B** form when L_1 = DMSO (model for isolated compounds **6** and **7**) clearly throws out the result that the D4R form with DMSO as the ancillary ligand is the global minimum and is stabilized by an order of about 30 kJ/mol (Table 5). It is also interesting to note that an all-DMSO cubane is far more stabilized than an all-DMSO-coordinated octameric cluster ($L_1 = L_2$ = DMSO), as can been seen from entry 2 of Table 5.

Thus, the results of DFT calculations are in total agreement with the observed experimental pattern and the structures of the isolated products. On the basis of these results it is hypothesized that the presence of water at L_2 position triggers the opening of that Zn−O−P face and eventually results in dimerization.

3. CONCLUSIONS

Synthesis, characterization, and structural modulations of two series of hitherto unknown octanuclear zinc phosphates have been reported. The octanuclear zinc phosphates **2** and **3**, presumably formed by the fusion of two D4R zinc phosphates, are produced by the reaction of zinc acetate and halo-aryl phosphate with hydroxypyridine in acetonitrile, while the octanuclear zinc phosphates **4** and **5**, involving further scrambling/rearrangement of inorganic cores, are obtained by reaction with dihydroxypyridine. Interesting structural transformations have been observed for both series of octanuclear zinc phosphates, which convert to DMSO-decorated tetranuclear D4R zinc phosphates **6** and **7**. Reaction of tetramers **6** and **7** with hydroxypyridine in acetonitrile leads to simple DMSO substitution by hpy and no cluster fusion. Gas- and liquid-phase DFT calculations support formation of octamers **2** and **3** in acetonitrile compared to tetranuclear D4R zinc phosphates, which are obtained in methanol from the same starting materials. The calculations further support the reorganization of octanuclear zinc phosphates **2**−**5** to D4R tetranuclear complexes **6** and **7** in DMSO.

4. EXPERIMENTAL SECTION

4.1. Methods and Materials. All the reactions were carried under aerobic conditions without excluding moisture or oxygen. The melting points were measured in glass capillaries and are reported uncorrected. Infrared spectra were obtained on a Perkin-Elmer Spectrum One FT-IR spectrometer as KBr discs. Microanalyses were performed on a Thermo Finnigan (FLASH EA 1112) microanalyzer. NMR studies were performed on Bruker Avance DPX-400 and 500 MHz spectrometers. For CP-MAS NMR measurements, a 4.0 mm zircon rotor with a spin rate of ∼10 000 Hz at 295−300 K has been employed. Thermogravimetric analyses were carried out on a Perkin−Elmer Pyris thermal analysis system under a stream of nitrogen gas at a heating rate of 10 °C/min. The ESI-MS studies were carried out on a Bruker MaXis impact mass spectrometer. Solvents were purified according to standard procedures prior to use.[26] Commercially available starting materials such as $[Zn(OAc)_2{\cdot}2H_2O]$ (s.d. Fine), 2-hydroxypyridine (Lancaster), and 2,3-dihydroxypyridine (Lancaster) were used as procured. Syntheses of 4-chloro- and 4-bromo-2,6-diisopropylphenyl phosphate were carried out as per reported procedures.[27]

4.2. Calculations. Density functional theory was used to calculate the relative energy of the complexes. The systems were optimized using the B3LYP functional along with the LANL08+ basis set with effective core potentials (ECPs)[28] for the zinc and TZV from Ahlrichs and co-workers for the rest of the atoms. The actual complexes are quite large relative to the computational facility available, so the

DOI: 10.1021/acs.inorgchem.5b01308
Inorg. Chem. 2015, 54, 9458−9469

systems have been simplified by fixing 4-halo-2,6-diisopropyl phenoxy (OAr) groups with −OMe and 2-hydroxypyridine with MeOH, with no alterations in the inorganic cores. To account for the influence of solvent, the polarizable continuum model (PCM) was employed using the same level of theory on the optimized geometries. All the calculations were done using the Gaussian 09 suit of program along with the GAUSSVIEW-5 graphical interface. For the solvent phase calculations the dielectric constants (ε) for acetonitrile, methanol, and DMSO were taken as 35.688, 32.613, and 46.826 respectively.

4.3. Synthesis and Characterization of 2 and 3. To the solution of $[Zn(OAc)_2{\cdot}2H_2O]$ (0.055 g, 0.25 mmol) and Cl-dippH$_2$ (0.073 g, 0.25 mmol) or Br-dippH$_2$ (0.085 g, 0.25 mmol) in acetonitrile (30 mL) was added a solution of hpy (0.024 g, 0.25 mmol) in acetonitrile slowly. The resultant solution was filtered, and **2** and **3** were obtained as single crystals in a time of 1 week.

2. Mp: >250 °C. Yield: 0.055 g (66% based on Cl-dippH$_2$). Anal. Calcd for $C_{120}H_{158}Cl_8N_6O_{38}P_8Zn_8$ (M_r = 3330.0) (%): C, 43.06; H, 4.76; N, 2.51. Found: C, 43.59; H, 4.64; N, 2.53. IR (KBr, cm^{-1}): 3417 (m), 2964 (s), 1647 (s), 1609 (s), 1542 (m), 1465 (w), 1333 (s), 1039 (w), 1179 (s), 1022 (s), 922 (s), 830 (s), 778 (s), 573 (w). ^{1}H NMR (DMSO-d_6, 500 MHz): δ 11.54 (br, 4H, py-N$^+$-H), 7.42 (t, 4H, hpy, $^3J_{HH}$ = 4.4 Hz), 7.40 (d 4H, hpy, $^3J_{HH}$ = 4.4 Hz,), 7.02 (s, 16H, ArH), 6.31 (d, 4H, hpy, $^3J_{HH}$ = 9.2 Hz), 6.14 (t, $^3J_{HH}$ = 6.4 Hz, 4H, hpy), 3.63 (m, 16H, ^{i}Pr-CH $^3J_{H-H}$ = 6.8 Hz), 1.09 (d, $^3J_{H-H}$ = 6.8 Hz, 96H, CH$_3$) ppm. ^{31}P NMR (DMSO-d_6, 201 MHz): δ −5.4 ppm. TGA [temp range °C (% weight loss)]: 30−204 (∼3.0); 200−470 (∼58.5); 470−1027 (∼17.5).

3. Mp: >250 °C. Yield: 0.045 g (48% based on Br-dippH$_2$). Anal. Calcd for $C_{120}H_{158}Br_8N_6O_{38}P_8Zn_8$ (M_r = 3702.8) (%): C, 38.92; H, 4.20; N, 2.27. Found: C, 0.38.56; H, 4.39; N, 3.19. IR (KBr, cm^{-1}): 3128 (w), 2966 (s), 1646 (s), 1610 (s), 1542 (m), 1465 (w), 1333 (s), 1179 (s), 1020 (s), 918 (s), 806 (s), 774 (s), 535 (w). ^{1}H NMR (DMSO-d_6, 500 MHz): δ 11.54 (br, 4H, py-N$^+$-H), 7.42 (t, 4H, hpy, $^3J_{HH}$ = 4.4 Hz), 7.40 (d 4H, hpy, $^3J_{HH}$ = 4.4 Hz), 7.15 (s, 16H, ArH), 6.31 (d, 4H, hpy, $^3J_{HH}$ = 9.2 Hz), 6.15 (t, $^3J_{HH}$ = 6.4 Hz, 4H, hpy), 3.63 (m, 16H, ^{i}Pr-CH, $^3J_{H-H}$ = 6.8 Hz), 1.07 (d, $^3J_{H-H}$ = 6.8 Hz, 96H, CH$_3$) ppm. ^{31}P NMR (DMSO-d_6, 201 MHz): δ −5.5 ppm. TGA [temp range °C (% weight loss)]: 30−210 (∼4.0); 210−600 (∼57.5); 600−1000 (∼12.5).

4.4. Synthesis and Characterization of 4 and 5. To a solution of $[Zn(OAc)_2{\cdot}2H_2O]$ (0.055 g, 0.25 mmol) and Cl-dippH$_2$ (0.073 g, 0.25 mmol) or Br-dippH$_2$ (0.085 g, 0.25 mmol) in acetonitrile (30 mL) was slowly added a solution of dhpy (0.028 g, 0.25 mmol) in acetonitrile. The resultant solution was stirred for 2−3 h at room temperature and filtered to yield crystals of **4** and **5** in 1 week.

4. Mp: >250 °C. Yield: 0.045 g (54% based on Cl-dippH$_2$). Anal. Calcd for $C_{126}H_{162}Cl_8N_6O_{44}P_8Zn_8$ (M_r = 3335.19) (%): C, 42.61; H, 4.60; N, 2.37. Found: C, 42.14; H, 4.82; N, 2.44. IR (KBr, cm^{-1}): 3335 (m), 3262 (m), 3120 (m), 2966 (s), 2928 (m), 2870 (m), 2357 (br), 1603 (s), 1556 (m), 1453 (s), 1338 (s), 1161 (s), 1102 (s), 977 (s), 829 (s), 749 (s), 544 (s). ^{1}H NMR (DMSO-d_6, 500 MHz): δ 11.60 (br, 6H, py-N$^+$-H), 8.90 (s, 6H, py-OH, dhpy), 7.01 (s, 16H, ArH), 6.82 (d, 6H, dhpy, $^3J_{HH}$ = 6.0 Hz), 6.67 (d, 6H, dhpy, $^3J_{HH}$ = 6.8 Hz), 6.03 (t, 6H, dhpy, $^3J_{HH}$ = 6.0 Hz), 3.62 (m, 16H, ^{i}Pr-CH $^3J_{H-H}$ = 6.8 Hz), 1.08 (d, $^3J_{H-H}$ = 6.7 Hz, 96H, CH$_3$) ppm. ^{31}P NMR (DMSO-d_6, 201 MHz): δ −5.4 ppm. TGA [temp range °C (% weight loss)]: 30−200 (∼3.5); 200−450 (∼58.0); 450−1027 (∼25.0).

5. Mp: >250 °C. Yield: 0.040 g (43% based on Br-dippH$_2$). Anal. Calcd for $C_{126}H_{164}Br_8N_6O_{44}P_8Zn_8$ (M_r = 3690.80) (%): C, 37.75; H, 4.31; N, 1.52. Found: C, 38.15; H, 4.05 N, 1.69. IR (KBr, cm^{-1}): 3336 (m), 3250 (m), 3118 (m), 2965 (s), 2928 (m), 2870 (m), 2346 (br), 1647 (s), 1603 (s), 1555 (m), 1451 (s), 1337 (s), 1161 (s), 1101 (s), 977 (s), 804 (s), 749 (s), 543 (s). ^{1}H NMR (DMSO-d_6, 500 MHz): δ 11.60 (br, 6H, py-N$^+$-H), 8.90 (s, 6H, py-OH, dhpy), 7.16 (s, 16H, ArH), 6.82 (d, 6H, dhpy, $^3J_{HH}$ = 6.0 Hz,), 6.67 (d, 6H, dhpy, $^3J_{HH}$ = 6.8 Hz), 6.03 (t, 6H, dhpy, $^3J_{HH}$ = 6.0 Hz), 3.65 (m, 16H, ^{i}Pr-CH $^3J_{H-H}$ = 6.8 Hz), 1.07 (d, $^3J_{H-H}$ = 6.7 Hz, 96H, −CH$_3$) ppm. ^{31}P NMR (DMSO-d_6, 201 MHz): δ −5.5 ppm. TGA [temp range °C (% weight loss)]: 30−200 (∼2.0); 200−400 (∼51.5); 400−1050 (∼13.5).

4.5. Synthesis and Characterization of 6 and 7. About 0.500 g each of **2** (0.15 mmol) and **4** (0.13 mmol) were dissolved in 5 mL of DMSO separately, the solutions were filtered, and compound **6** was obtained as block-shaped crystals in both the solutions, after a time period of 1 week. Similarly, compounds **3** and **5** when recrystallized from a DMSO solution yielded **7** as single crystals.

6. Mp: >250 °C. Yield: 0.360 g (∼70%). Anal. Calcd for $C_{56}H_{88}Cl_4O_{20}P_4S_4Zn_4$ (M_r = 1736.23) (%): C, 38.72; H, 5.11; S, 7.38. Found: C, 38.65; H, 5.11; S, 7.13. IR (KBr, cm^{-1}): 3432 (m), 2968 (s), 2925 (m), 2870 (m), 1647 (s), 1587 (s), 1466 (w), 1336(s), 1338 (s), 1184 (w), 1023 (s), 922 (m), 827 (s), 779 (m), 693 (m), 547 (w). ^{1}H NMR (DMSO-d_6, 500 MHz): δ 7.02 (s, 8H, ArH), 3.63 (m, 8H, ^{i}Pr-CH, $^3J_{H-H}$ = 6.8 Hz), 1.09 (d, $^3J_{H-H}$ = 6.8 Hz, 48H, CH$_3$) ppm. ^{31}P NMR (DMSO-d_6, 201 MHz): δ −5.4 ppm. TGA [temp range °C (% weight loss)]: 30−200 (∼3.0); 200−450 (∼50.5); 450−1027 (∼15.0). ESI-MS: m/z calcd 1736.95, found 1736.96 [M]$^+$.

7. Mp: >250 °C. Yield: 0.400 g (∼60%). Anal. Calcd for $C_{64}H_{112}Br_4O_{24}P_4S_8Zn_4$ (M_r = 2227.23) (%): C, 34.51; H, 5.07; S, 11.52. Found: C, 34.54; H, 4.64; S, 9.92. IR (KBr, cm^{-1}): 3432 (m), 2960 (s), 2925 (s), 2869 (w), 1742 (m), 1610 (w), 1465 (m), 1338 (s), 1184 (s), 1023 (s), 913 (s), 803 (s), 779 (s), 541 (w). ^{1}H NMR (DMSO-d_6, 500 MHz): δ 7.15 (s, 8H, ArH), 3.63 (m, 8H, ^{i}Pr-CH $^3J_{H-H}$ = 6.8 Hz), 1.07 (d, $^3J_{H-H}$ = 6.8 Hz, 48H, CH$_3$) ppm. ^{31}P NMR (DMSO-d_6, 201 MHz): δ −5.5 ppm. TGA [temp range °C (% weight loss)]: 30−200 (∼7.0); 200−450 (∼52.5); 450−1027 (∼14.0). ESI-MS: m/z calcd 1914.76, found 1914.75 [M]$^+$.

4.6. Synthesis and Characterization of 8 and 9. To the stirred solutions of **6** (0.087 g, 0.05 mmol) and **7** (0.113 g, 0.05 mmol) in acetonitrile was added solid hpy ligand (0.047 g, 0.20 mmol). The resultant clear solutions were filtered and yielded crystals of **8** and **9**, respectively, in 2−3 days time.

8. Mp: >250 °C. Yield: 0.060 g (66% based on **6**). Anal. Calcd for $C_{68}H_{84}Cl_4N_4O_{20}P_4Zn_4$ (M_r 1804.76) (%): C, 44.68; H, 4.63; N, 3.07. Found: C, 43.95; H, 4.64; N, 2.53. IR (KBr, cm^{-1}): 3267 (m), 3141 (m), 2964 (s), 2868 (s), 1654 (s), 1602 (s), 1543 (m), 1418 (w), 1336 (s), 1183 (s), 1015 (s), 926 (s), 805 (s), 776 (s), 690 (s), 569 (s). ^{1}H NMR (DMSO-d_6, 500 MHz): δ 11.54 (br, 4H, py-N$^+$-H), 7.42 (t, 4H, 2-hpy, $^3J_{HH}$ = 4.4 Hz), 7.40 (d 4H, 2-hpy, $^3J_{HH}$ = 4.4 Hz,), 7.02 (s, 8H, ArH), 6.31 (d, 4H, 2-hpy, $^3J_{HH}$ = 9.2 Hz), 6.14 (t, $^3J_{HH}$ = 6.4 Hz, 4H, 2-hpy), 3.63 (m, 8H, ^{i}Pr-CH $^3J_{H-H}$ = 6.8 Hz), 1.09 (d, $^3J_{H-H}$ = 6.8 Hz, 48H, CH$_3$) ppm. ^{31}P NMR (DMSO-d_6, 201 MHz): δ −5.5 ppm. TGA [temp range °C (% weight loss)]: 30−200 (∼3.0); 200−450 (∼55.5); 470−1050 (∼17.5). ESI-MS (CH$_3$CN): m/z calcd [M] = 1804.76, found 1805.11, [M + H]$^+$; 1827.10, [M + Na]$^+$.

9. Mp: >250 °C. Yield: 0.045 g (46% based on **7**). Anal. Calcd for $C_{68}H_{84}Br_4N_4O_{20}P_4Zn_4$ (M_r = 1982.56) (%): C, 41.20; H, 4.27; N, 2.83. Found: C, 41.10; H, 4.25; N, 2.44. IR (KBr, cm^{-1}): 3269 (w), 3175 (w), 2966 (s), 2870 (w), 1651 (s), 1610 (s), 1543 (m), 1463 (w), 1384 (s), 1335 (s), 1182 (s), 1017 (s), 922 (s), 804 (s), 776 (s), 542 (w). ^{1}H NMR (DMSO-d_6, 500 MHz): δ 11.54 (br, 4H, py-N$^+$-H), 7.42 (t, 4H, 2-hpy, $^3J_{HH}$ = 4.4 Hz), 7.40 (d, 4H, 2-hpy, $^3J_{HH}$ = 4.4 Hz,), 7.15 (s, 8H, ArH), 6.31 (d, 4H, 2-hpy, $^3J_{HH}$ = 9.2 Hz), 6.15 (t, $^3J_{HH}$ = 6.4 Hz, 4H, 2-hpy), 3.63 (m, 8H, ^{i}Pr-CH $^3J_{H-H}$ = 6.8 Hz), 1.07 (d, $^3J_{H-H}$ = 6.8 Hz, 48H, CH$_3$) ppm. ^{31}P NMR (DMSO-d_6, 201 MHz): δ −5.4 ppm. TGA [temp range °C (% weight loss)]: 30−200 (∼4.0); 210−600 (∼58.0); 600−1050 (∼12.0). ESI-MS (CH$_3$CN): m/z calcd [M] = 1982.56, found 2004.97, [M + Na]$^+$.

4.7. Single-Crystal X-ray Diffraction Studies. The single crystals of compounds **2**−**9** were directly obtained from the reaction mixture and mounted in paraffin oil on a Rigaku Saturn 724+ ccd diffractometer for unit cell determination and three-dimensional intensity data collection. Data integration and indexing were done using crystal clear, and structures were solved using the direct method SIR-92.[29] The complete refinement calculations were carried using programs in the WinGX module.[30] The final refinement of structures was carried out using full-scan least-squares methods on F^2 using SHELXL-97.[31] Owing to the high R values obtained for compounds **3**, **4**, and **5**, recrystallization of the samples followed by remeasurement of intensity data was attempted multiple times albeit with no major improvement. The high R values can be attributed to extremely weak

DOI: 10.1021/acs.inorgchem.5b01308
Inorg. Chem. 2015, 54, 9458−9469

Table 6. Crystallographic Details of Compounds 2−9

	2	3	4	5	6	7	8	9
identification code	AJZ-478	AJZ-935	AJZ-243	AJZ-806	AJZ-844	AJZ-733	AJZ-623	AJZ-903
empirical formula	$C_{120}H_{158}Cl_8N_6O_{38}P_8Zn_8$	$C_{120}H_{158}Br_8N_6O_{38}P_8Zn_8$	$C_{130}H_{162}Cl_8N_8O_{46}P_8Zn_8$	$C_{126}H_{166}Br_8N_6O_{48}P_8Zn_8$	$C_{56}H_{88}Cl_4O_{20}P_4S_4Zn_4$	$C_{64}H_{112}Br_4O_{24}P_4S_8Zn_4$	$C_{68}H_{84}Cl_4N_4O_{20}P_4Zn_4$	$C_{68}H_{84}Br_4N_4O_{20}P_4Zn_4$
AJZ-944	3340.80	3702.61	3626.99	3938.62	1736.75	2227.02	1804.55	1982.39
temp [K]	150(2)	150(2)	150(2)	150(2)	150(2)	150(2)	150(2)	150(2)
cryst syst	tetragonal	tetragonal	orthorhombic	orthorhombic	monoclinic	monoclinic	monoclinic	monoclinic
space group	$I4_1/a$	$I4_1/a$	*Pbca*	*Pbca*	*I*2/*a*	*P*2/*c*	*I*2/*a*	*I*2/*a*
a [Å]	43.5493(11)	43.962(2)	21.993(4)	21.872(9)	31.733(4)	31.221(4)	17.828(4)	17.827(5)
b [Å]	43.5493(11)	43.962(2)	24.211(5)	23.851(9)	14.8847(15)	15.0144(18)	22.866(4)	23.067(6)
c [Å]	16.3262(7)	16.4549(1)	29.741(7)	30.092(12)	35.418(3)	20.073(2)	21.186(4)	21.210(5)
α [deg]								
β [deg]					112.669(8)	95.027(3)	96.233(14)	95.394(19)
γ [deg]								
V [Å^3]	30963.3(2)	31802(3)	15836(6)	15698(1)	15437(3)	9373.3(19)	8585(2)	8683(4)
Z	8	8	4	4	8	4	4	4
D(calcd) [Mg/m^3]	1.433	1.547	1.521	1.667	1.494	1.578	1.396	1.516
μ [mm^{-1}]	1.509	3.345	1.486	3.399	1.620	3.027	1.368	3.070
θ range [deg]	2.58 to 25.00	2.56 to 25.00	2.59 to 25.00	2.53 to 25.00	2.69 to 25.248	2.52 to 25.00	2.555 to 25.498	2.615 to 25.500
no. of reflns collected	110 535	95 913	117 025	115 395	58 613	69 983	33 747	34 167
indep reflns	13 628	14 004	13 930	13 796	13 914	16 459	7992	8080
data/restraints/params	13 628/6/855	14 004/2/874	13 930/20/942	13 796/3/927	13 914/6/839	16 459/0/975	7992/0/469	8080/0/469
GOF	1.065	1.294	1.528	1.373	1.079	1.152	1.205	1.177
R1($I_o > 2\sigma(I_o)$)	0.0672	0.1150	0.1603	0.1264	0.0451	0.0720	0.0439	0.0538
wR2(all data)	0.1814	0.2198	0.2733	0.2157	0.1067	0.1298	0.0931	0.0968

DOI: 10.1021/acs.inorgchem.5b01308
Inorg. Chem. 2015, 54, 9458−9469

diffracting ability of the very small size of the crystal obtained for all three compounds (**3**: 0.10 × 0.04 × 0.03 mm, **4**: 0.08 × 0.04 × 0.03 mm; **5**: 0.08 × 0.04 × 0.03 mm), apart from the apparent deterioration of crystal quality when taken out of the solvent. Diffuse and weak residual electron density corresponding to the solvent molecules in the lattice of compounds **2**, **8**, and **9** could not be modeled appropriately and hence has been squeezed toward the end of the refinement. The assignment of the solvent to these compounds has been done on the basis of elemental analyses, TGA, and solvent-accessible volume values. The crystal data and refinement details of all the crystal structure are listed in Table 6.

■ ASSOCIATED CONTENT

Supporting Information

The Supporting Information is available free of charge on the ACS Publications website at DOI: 10.1021/acs.inorgchem.5b01308.

Crystallographic data of **2** [CCDC 1400202], **3** [CCDC 1400203], **4** [CCDC 1400204], **5** [CCDC 1400205], **6** [CCDC 1400206], **7** [CCDC 1400207], **8** [CCDC 1400208], and **9** [CCDC 1400209] (CIF)

Synthesis, crystallographic details, additional figures, and spectral characterization (PDF)

■ AUTHOR INFORMATION

Corresponding Author

*Tel (R. Murugavel): +91 22 2576 7163. Fax: +91 22 2572 3480. E-mail: rmv@chem.iitb.ac.in.

Notes

The authors declare no competing financial interest.

■ ACKNOWLEDGMENTS

This work was supported by SERB and DST Nanomission, New Delhi, and DAE (BRNS), Mumbai. R.M. thanks BRNS for the award of DAE-SRC Outstanding Investigator Award, which enabled the purchase of a single-crystal CCD diffractometer. A.A.D. thanks UGC for a research fellowship.

■ DEDICATION

Dedicated to Professor S. S. Krishnamurthy on the occasion of his 75th birthday.

■ REFERENCES

(1) Wilson, S. T.; Lok, B. M.; Messina, C. A.; Cannan, T. R.; Flanigen, E. M. J. *J. Am. Chem. Soc.* **1982**, *104*, 1146. (b) Murugavel, R.; Walawalkar, M. G.; Pothiraja, R.; Rao, C. N. R.; Choudhury, A. *Chem. Rev.* **2008**, *108*, 3549.

(2) Metallophosphates as catalysts: (a) Ma, T. Y.; Zhang, X. J.; Yuan, Z. Y. *Microporous Mesoporous Mater.* **2009**, *123*, 234. (b) Hutchings, G. J. *J. Mater. Chem.* **2004**, *14*, 3385. (c) Muneyama, E.; Kunishige, A.; Ohdan, K.; Ai, M. *J. Catal.* **1996**, *158*, 378. (d) Wang, Y.; Wang, X. X.; Su, Z.; Guo, Q.; Tang, Q. H.; Zhang, Q. H.; Wan, H. L. *Catal. Today* **2004**, *93*, 155. (e) Lin, R. H.; Ding, Y. J.; Gong, L. F.; Dong, W. D.; Wang, J. H.; Zhang, T. *J. Catal.* **2010**, *272*, 65. (f) Kamiya, Y.; Nishikawa, E.; Satsuma, A.; Yoshimune, M.; Okuhara, T. *Microporous Mesoporous Mater.* **2002**, *54*, 277. (g) Alberti, G.; Casciola, M.; Marmottini, F.; Vivani, R. *J. Porous Mater.* **1999**, *6*, 299. (h) Kleitz, F.; Thomson, S. J.; Liu, Z.; Terasaki, O.; Schuth, F. *Chem. Mater.* **2002**, *14*, 4134. (i) Yuan, Z. Y.; Ren, T. Z.; Azioune, A.; Pireaux, J. J.; Su, B. L. *Catal. Today* **2005**, *105*, 647. (j) Yu, J.; Wang, A.; Tan, J.; Li, X.; van Bokhoven, J. A.; Hu, Y. K. *J. Mater. Chem.* **2008**, *18*, 3601. (k) Sarkar, A.; Pramanik, P. *Microporous Mesoporous Mater.* **2009**, *117*, 580.

(3) Ion exchangers: (a) Alvarez, C.; Llavona, R.; Garcia, J. R.; Suarez, M.; Rodriguez, J. *Inorg. Chem.* **1987**, *26*, 1045. (b) Shah, B.; Chudasama, U. *Desalin. Water Treat.* **2012**, *38*, 227. (c) Bhaumik, A.; Inagaki, S. *J. Am. Chem. Soc.* **2001**, *123*, 691.

(4) Adsorbants: (a) Katz, H. E.; Scheller, G.; Putvinski, T. M.; Schilling, M. L.; Wilson, W. L.; Chidsey, C. E. D. *Science* **1991**, *254*, 1485. (b) Li, X. S.; Courtney, A. R.; Yantasee, W.; Mattigod, S. V.; Fryxell, G. E. *Inorg. Chem. Commun.* **2006**, *9*, 293. (c) Dutta, A.; Patra, A. K.; Bhaumik, A. *Microporous Mesoporous Mater.* **2012**, *155*, 208. (d) Kandori, K.; Nakashima, H.; Ishikawa, T. *J. Colloid Interface Sci.* **1993**, *160*, 499.

(5) Electronic devices: (a) Padhi, A. K.; Nanjundaswamy, K. S.; Masquelier, C.; Okada, S.; Goodenough, J. B. *J. Electrochem. Soc.* **1997**, *144*, 1609. (b) Tian, X. Y.; He, W.; Cui, J. J.; Zhang, X. D.; Zhou, W. J.; Yan, S. P.; Sun, X. N.; Han, X. X.; Han, S. S.; Yue, Y. Z. *J. Colloid Interface Sci.* **2010**, *343*, 344. (c) Qian, L. C.; Xia, Y.; Zhang, W. K.; Huang, H.; Gan, Y. P.; Zeng, H. J.; Tao, X. Y. *Microporous Mesoporous Mater.* **2012**, *152*, 128.

(6) Photoluminescence: (a) Rodriguez-Liviano, S.; Aparicio, F. J.; Rojas, T. C.; Hungria, A. B.; Chinchilla, L. E.; Ocana, M. *Cryst. Growth Des.* **2012**, *12*, 635. (b) Luo, Q. L.; Shen, S. D.; Lu, G. Z.; Xiao, X. Z.; Mao, D. S.; Wang, Y. Q. *J. Mater. Chem.* **2009**, *19*, 8079. (c) Ren, T. Z.; Yuan, Z. Y.; Azioune, A.; Pireaux, J. J.; Su, B. L. *Langmuir* **2006**, *22*, 3886.

(7) Medicine: (a) Kononova, S. V.; Nesmeyanova, M. A. *Biochemistry (Moscow)* **2002**, *67*, 184. (b) Gielen, M.; Tiekink, E. R. T. Metallotherapeutic Drugs and Metal-Based Diagnostic Agents. In *The Use Of Metals In Medicine*; John Wiley & Sons, Ltd., 2005. (c) Kim, T. W.; Chung, P. W.; Slowing, I. I.; Tsunoda, M.; Yeung, E. S.; Lin, V. S. Y. *Nano Lett.* **2008**, *8*, 3724. (d) Liu, J. W.; Stace-Naughton, A.; Jiang, X. M.; Brinker, C. J. *J. Am. Chem. Soc.* **2009**, *131*, 1354.

(8) Proton conduction: (a) Nishiyama, Y.; Tanaka, S.; Hillhouse, H. W.; Nishiyama, N.; Egashira, Y.; Ueyama, K. *Langmuir* **2006**, *22*, 9469. (b) Tian, B. Z.; Liu, X. Y.; Tu, B.; Yu, C. Z.; Fan, J.; Wang, L. M.; Xie, S. H.; Stucky, G. D.; Zhao, D. Y. *Nat. Mater.* **2003**, *2*, 159. (c) Sahu, A. K.; Pitchumani, S.; Sridhar, P.; Shukla, A. K. *Fuel Cells* **2009**, *9*, 139. (d) Jimenez-Jimenez, J.; Maireles-Torres, P.; Olivera-Pastor, P.; Rodriguez-Castellon, E.; Jimenez-Lopez, A.; Jones, D. J.; Roziere, J. *Adv. Mater.* **1998**, *10*, 812. (e) Rodriguez-Castellon, E.; Jimenez-Jimenez, J.; Jimenez-Lopez, A.; Maireles-Torres, P.; Ramos-Barrado, J. R.; Jones, D. J.; Roziere, J. *Solid State Ionics* **1999**, *125*, 407.

(9) Gas storage and magnetism: (a) Kalita, A. C.; Gogoi, N.; Jangir, R.; Kuppuswamy, S.; Walawalkar, M. G.; Murugavel, R. *Inorg. Chem.* **2014**, *53*, 8959. (b) Gupta, S. K.; Dar, A. A.; Rajeshkumar, T.; Kuppuswamy, S.; Langley, S. K.; Murray, K. S.; Rajaraman, G.; Murugavel, R. *Dalton Trans.* **2015**, *44*, 5961. (c) Konar, S.; Mukherjee, P. S.; Zangrando, E.; Lloret, F.; Ray Chaudhuri, N. *Angew. Chem., Int. Ed.* **2002**, *41*, 1561.

(10) Gier, T. E.; Stucky, G. D. *Nature* **1991**, *349*, 508.

(11) (a) Cheetham, A. K.; Férey, G.; Loiseau, T. *Angew. Chem., Int. Ed.* **1999**, *38*, 3268. (b) Rao, C. N. R.; Natarajan, S.; Choudhury, A.; Neeraj, S.; Ayi, A. A. *Acc. Chem. Res.* **2001**, *34*, 80. (c) Finn, R. C.; Zubieta, J.; Haushalter, R. C. *Prog. Inorg. Chem.* **2002**, *51*, 421−601. (d) Clearfield, A. *Prog. Inorg. Chem.* **1997**, *47*, 371. (e) Cao, G.; Hong, H.-G.; Mallouk, T. E. *Acc. Chem. Res.* **1992**, *25*, 420.

(12) (a) Katovic, A.; Giordano, G.; Kowalak, S. *Stud. Surf. Sci. Catal.* **2002**, *142*, 39. (b) Tischendorf, B. C.; Alam, T. M.; Cygan, R. T.; Otaigbe, J. U. *J. Non-Cryst. Solids* **2003**, *316*, 261. (c) Simon-Masseron, A.; Paillaud, J. L.; Patarin, J. *Chem. Mater.* **2003**, *15*, 1000. (d) Lin, Z. E.; Yao, Y. W.; Zhang, J.; Yang, G. Y. *J. Chem. Soc., Dalton Trans.* **2002**, 4527. (e) Chen, X. M.; Zhao, Y. N.; Wang, R. J.; Ming, L. A.; Mai, Z. H. *J. Chem. Soc., Dalton Trans.* **2002**, 3092. (f) Liu, Y. L.; Liu, W.; Xing, Y.; Shi, Z.; Fu, Y. L.; Pang, W. Q. *J. Solid State Chem.* **2002**, *166*, 265. (g) Jensen, T. R.; Hazell, R. G.; Christensen, A. N.; Hanson, J. C. *J. Solid State Chem.* **2002**, *166*, 341. (h) Zhao, Y. N.; Ju, J.; Chen, X. M.; Li, X. H.; Wang, Y.; Wang, R. J.; Li, M.; Mai, Z. H. *J. Solid State Chem.* **2002**, *166*, 369. (i) Zhao, Y. N.; Yao, Y. W.; Li, X. H.; Chen, X. M.; Li, M.; Mai, Z. H. *Chem. Lett.* **2002**, 542. (j) Natarajan, S. *J. Chem. Soc., Dalton Trans.* **2002**, 2088.

DOI: 10.1021/acs.inorgchem.5b01308
Inorg. Chem. 2015, 54, 9458−9469

(13) (a) Bu, X.; Feng, P.; Gier, T. E.; Stucky, G. D. *J. Solid State Chem.* **1998**, *136*, 210. (b) Feng, P.; Bu, X.; Stucky, G. D. *Angew. Chem., Int. Ed. Engl.* **1995**, *34*, 1745. (c) Gier, T. E.; Stucky, G. D. *Nature* **1991**, *349*, 508. (d) Nenoff, T. M.; Harrison, W. T. A.; Gier, T. E.; Stucky, G. D. *J. Am. Chem. Soc.* **1991**, *113*, 378. (e) Harrison, W. T. A.; Gier, T. E.; Moran, K. L.; Nicol, J. M.; Eckert, H.; Stucky, G. D. *Chem. Mater.* **1991**, *3*, 27. (f) Song, T.; Xu, J.; Zhao, Y.; Yue, Y.; Xu, Y.; Xu, R.; Hu, N.; Wei, G.; Jia, H. *J. Chem. Soc., Chem. Commun.* **1994**, 1171.

(14) Harrison, W. T. A.; Gier, T. E.; Stucky, G. D.; Broach, R. W.; Bedard, R. A. *Chem. Mater.* **1996**, *8*, 145.

(15) (a) Harrison, W. T. A.; Hannooman, L. *Angew. Chem., Int. Ed. Engl.* **1997**, *36*, 640. (b) Harrison, W. T. A.; Hannooman, L. *J. Solid State Chem.* **1997**, *131*, 363. (c) Harrison, W. T. A.; Phillips, M. L. F. *Chem. Commun.* **1996**, 2771. (d) Harrison, W. T. A.; Phillips, M. L. F. *Chem. Mater.* **1997**, *9*, 1837.

(16) (a) Lugmair, C. G.; Tilley, T. D.; Rheingold, A. L. *Chem. Mater.* **1997**, *9*, 339. (b) Yang, Y.; Pinkas, J.; Noltemeyer, M.; Roesky, H. W. *Inorg. Chem.* **1998**, *37*, 6404. (c) Anantharaman, G.; Chandrasekhar, V.; Walawalkar, M. G.; Roesky, H. W.; Vidovic, D.; Magull, J.; Noltemeyer, M. *J. Chem. Soc., Dalton Trans.* **2004**, 1271−1275. (d) Yang, Y.; Pinkas, J.; Roesky, H. W.; Schäfer, M. *Angew. Chem., Int. Ed.* **1998**, *37*, 2650. (e) Chandrasekhar, V.; Sasikumar, P.; Senapati, T.; Dey, A. *Inorg. Chim. Acta* **2010**, *363*, 2920. (f) Chyba, J.; Moravec, Z.; Necas, M.; Mathur, S.; Pinkas, J. *Inorg. Chem.* **2014**, *53*, 3753.

(17) Ayi, A. A.; Choudhury, A.; Natarajan, S.; Rao, C. N. R. *J. Mater. Chem.* **2000**, *10*, 2606. (b) Natarajan, S.; van Wullen, L.; Klein, W.; Jansen, M. *Inorg. Chem.* **2003**, *42*, 6265.

(18) (a) Harrison, W. T. A.; Broach, R. W.; Bedard, R. A.; Gier, T. E.; Bu, X.; Stucky, G. D. *Chem. Mater.* **1996**, *8*, 691. (b) Gupta, S. K.; Kuppuswamy, S.; Walsh, J. P. S.; Mclnnes, E. J. L.; Murugavel, R. *Dalton Trans.* **2015**, *44*, 5587.

(19) (a) Murugavel, R.; Kuppuswamy, S.; Gogoi, N.; Boomishankar, R.; Steiner, A. *Chem. - Eur. J.* **2010**, *16*, 994. (b) Murugavel, R.; Kuppuswamy, S.; Maity, A. N.; Singh, M. P. *Inorg. Chem.* **2009**, *48*, 183. (c) Murugavel, R.; Gogoi, N. *J. Organomet. Chem.* **2010**, *695*, 916. (d) Murugavel, R.; Kuppuswamy, S.; Gogoi, N.; Steiner, A.; Bacsa, J.; Boomishankar, R.; Suresh, K. G. *Chem. - Asian J.* **2009**, *4*, 143. (e) Murugavel, R.; Kuppuswamy, S.; Gogoi, N.; Steiner, A. *Inorg. Chem.* **2010**, *49*, 2153. (f) Dar, A. A.; Sharma, S. K.; Murugavel, R. *Inorg. Chem.* **2015**, *54*, 4882.

(20) (a) Ziegler, M. L.; Weiss, J. *Angew. Chem.* **1970**, *82*, 931; *Angew. Chem., Int. Ed. Engl.* **1970**, *9*, 905. (b) Ishimori, M.; Hagiwara, T.; Tsuruta, T.; Kai, Y.; Yasuoka, N.; Kasai, N. *Bull. Chem. Soc. Jpn.* **1976**, *49*, 1165. (c) Attanasio, D.; Dessy, G.; Fares, V. *J. Chem. Soc., Dalton Trans.* **1979**, 28. (d) Lalioti, N.; Raptopoulou, C. P.; Terzis, A.; Aliev, A. E.; Perlepes, S. P.; Gerothanassis, I. P.; Manessi-Zoupa, E. *Chem. Commun.* **1998**, 1513. (e) Tesmer, M.; Mueller, B.; Vahrenkamp, H. *Chem. Commun.* **1997**, 721.

(21) Yang, Y.; Pinkas, J.; Noltemeyer, M.; Schmidt, H.-G.; Roesky, H. W. *Angew. Chem., Int. Ed.* **1999**, *38*, 664.

(22) (a) Mason, M. R.; Perkins, A. M.; Matthews, R. M.; Fisher, J. D.; Mashuta, M. S.; Vij, A. *Inorg. Chem.* **1998**, *37*, 3734. (b) Walawalkar, M. G.; Roesky, H. W.; Murugavel, R. *Acc. Chem. Res.* **1999**, *32*, 117−126. (c) Fu, R.; Hu, S.; Wu, X. *Dalton Trans.* **2009**, 9440.

(23) Coxall, R. A.; Harris, S. G.; Henderson, D. K.; Parsons, S.; Tasker, P. A.; Winpenny, R. E. P. *J. Chem. Soc., Dalton Trans.* **2000**, 2349.

(24) Gamoke, B.; Neff, D.; Simons, J. *J. Phys. Chem. A* **2009**, *113*, 5677.

(25) (a) Murugavel, R.; Kuppuswamy, S.; Boomishankar, R.; Steiner, A. *Angew. Chem., Int. Ed.* **2006**, *45*, 5536. (b) Kalita, A. C.; Roch-Marchal, C.; Murugavel, R. *Dalton Trans.* **2013**, *42*, 9755. (c) Kalita, A. C.; Murugavel, R. *Inorg. Chem.* **2014**, *53*, 3345.

(26) Furniss, B. S.; Hannaford, A. J.; Tatchell, A. R.; Smith, P. W. G. *Vogel's, Text Book of Practical Organic Chemistry*, 5th ed.; Longman Scientific and Technical: Harlow, UK, 1989.

(27) Dar, A. A.; Mallick, A.; Murugavel, R. *New J. Chem.* **2015**, *39*, 1186.

(28) (a) Hay, P. J.; Wadt, W. R. *J. Chem. Phys.* **1985**, *82*, 299. (b) Roy, L. E.; Hay, P. J.; Martin, R. L. *J. Chem. Theory Comput.* **2008**, *4*, 1029.

(29) Altomare, A.; Cascarano, G.; Giacovazzo, C.; Guagliardi, A. *J. Appl. Crystallogr.* **1993**, *26*, 343.

(30) Farrugia, L. J. *J. Appl. Crystallogr.* **1999**, *32*, 837.

(31) Sheldrick, G. M. *Acta Crystallogr., Sect. A: Found. Crystallogr.* **2008**, *A64*, 112.

DOI: 10.1021/acs.inorgchem.5b01308
Inorg. Chem. 2015, 54, 9458−9469